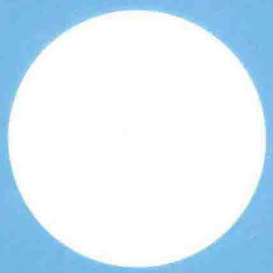

Vascular Biochemistry

edited by

Peter Zahradka,
Jeffrey Wigle and
Grant N. Pierce

Kluwer Academic Publishers

Vascular Biochemistry

Edited by

PETER ZAHRADKA

St. Boniface General Hospital
Research Center
351 Tache Avenue
R2H 2A6, Winnipeg, Manitoba
Canada

JEFFREY WIGLE

Institute of Cardiovascular Sciences
St. Boniface General Hospital
351 Tache Avenue
R2H 2A6, Winnipeg, Manitoba
Canada

GRANT N. PIERCE

Division of Stroke & Vascular Disease
St. Boniface General Hospital
Research Center
Faculty of Medicine, University of Manitoba
R2H 2A6, Winnipeg, Manitoba
Canada

Reprinted from *Molecular and Cellular Biochemistry*, Volume 246 (2003)

Kluwer Academic Publishers
Dordrecht / Boston / London

Distributors for North, Central and South America:
Kluwer Academic Publishers
101 Philip Drive
Assinippi Park
Norwell, Massachusetts 02061 USA
Telephone (781) 871-6600
Fax (781) 681-9045
E-mail <kluwer@wkap.com>

Distributors for all other countries:
Kluwer Academic Publishers Group
Distribution Centre
Post Office Box 322
3300 AH Dordrecht, The Netherlands
Telephone 31 78 6392 392
Fax 31 78 6546 474
E-mail <services@wkap.nl>

 Electronic Services <http://www.wkap.nl>

Library of Congress Cataloging-in-Publication Data

A C.I.P. Catalogue record for this book is available from the Library of Congress

ISBN 1-4020-7398-4

Printed on acid-free paper

Printed in The Netherlands

VASCULAR BIOCHEMISTRY

Molecular and Cellular Biochemistry:

An International Journal for Chemical Biology in Health and Disease

CONTENTS VOLUME 246, Nos. 1 & 2, April 2003

VASCULAR BIOCHEMISTRY

Drs. Peter Zahradka, Jeffrey Wigle and Grant N. Pierce

Preface 1

B. Fernández, A. Kampmann, F. Pipp, R. Zimmermann and W. Schaper: Osteoglycin expression and localization in rabbit tissues and atherosclerotic plaques 3–11

A. Aires Ferreira Rodrigues Borges and O. Moreira Gomes: Effects of midazolam on the contraction and relaxation of segments of thoracic aorta stripped of endothelium and stimulated by adrenaline – experimental study in rabbits 13–17

D. Bia, J.C. Grignola, R.L. Armentano and F.F. Ginés: Improved pulmonary artery buffering function during phenylephrine-induced pulmonary hypertension 19–24

J. Tarchalski, P. Guzik and H. Wysocki: Correlation between the extent of coronary atherosclerosis and lipid profile 25–30

Y.J. Jiang, B. Lu, P.C. Choy and G.M. Hatch: Regulation of cytosolic phospholipase A_2, cyclooxygenase-1 and -2 expression by PMA, TNFα, LPS and M-CSF in human monocytes and macrophages 31–38

S. Maruyama, K. Kato, M. Kodama, Y. Okura, S. Hirono, K. Fuse, H. Hanawa, O. Nakagawa, M. Nakazawa, T. Miida, E. Yaoita, T. Yamamoto, I. Inoue and Y. Aizawa: FR167653 suppresses the progression of experimental autoimmune myocarditis 39–44

P. Ostadal, D. Alan, P. Hajek, D. Horak, J. Vejvoda, J. Trefanec, M. Mates and J. Vojacek: The effect of early treatment by cerivastatin on the serum level of C-reactive protein, interleukin-6, and interleukin-8 in the patients with unstable angina and non-Q-wave myocardial infarction 45–50

M. Franco, G. Castro, L. Romero, J.C. Regalado, A. Medina, C. Huesca-Gómez, S. Ramírez, L.F. Montaño, C. Posadas-Romero and O. Pérez-Méndez: Decreased activity of lecithin:cholesterol acyltransferase and hepatic lipase in chronic hypothyroid rats: Implications for reverse cholesterol transport 51–56

D. Scholz, S. Thomas, S. Sass and T. Podzuweit: Angiogenesis and myogenesis as two facets of inflammatory post-ischemic tissue regeneration 57–67

G.X. Shen: Impact and mechanism for oxidized and glycated lipoproteins on generation of fibrinolytic regulators from vascular endothelial cells 69–74

R.B. Singh, N.S. Neki, K. Kartikey, D. Pella, A. Kumar, M.A. Niaz and A.S. Thakur: Effect of coenzyme Q10 on risk of atherosclerosis in patients with recent myocardial infarction 75–82

D.H. Morris: Methodologic challenges in designing clinical studies to measure differences in the bioequivalence of n-3 fatty acids 83–90

S. Hirono and G.N. Pierce: Dissemination of *Chlamydia pneumoniae* to the vessel wall in atherosclerosis 91–95

M. Chen, L.Y. Li and Y.-P. Qi: Bcl10 protein can act as a transcription activator in yeast 97–103

P. Zahradka, N. Yurkova, B. Litchie, M.C. Moon, D.F. Del Rizzo and C.G. Taylor: Activation of peroxisome proliferator-activated receptors α and γ1 inhibits human smooth muscle cell proliferation 105–110

C.J.A. Hirst, M. Herlyn, P.A. Cattini and E. Kardami: High levels of CUG-initiated FGF-2 expression cause chromatin compaction, decreased cardiomyocyte mitosis, and cell death 111–116

S. Asgary, G.H. Naderi, N. Sarrafzadegan and M. Gharypur: *In vitro* effect of nicotine and cotinine on the susceptibility of LDL oxidation and hemoglobin glycosylation 117–120

M.J.B. Kutryk and B. Ramjiawan: Plasmid lipid and lipoprotein pattern in the Inuit of the Keewatin district of the Northwest territories 121–127

R.M. Levin, A. Borow, S.S. Levin and N. Haugaard: Effect of DHLA on response of isolated rat urinary bladder to repetitive field stimulation 129–135

M.L. Dubey, R. Hegde, N.K. Ganguly and R.C. Mahajan: Decreased level of 2,3-diphosphoglycerate and alteration of structural integrity in erythrocytes infected with *Plasmodium falciparum in vitro* 137–141

Y. Duraisamy, J. Gaffney, M. Slevin, C.A. Smith, K. Williamson and N. Ahmed: Aminosalicylic acid reduces the antiproliferative effect of hyperglycaemia, advanced glycation endproducts and glycated basic fibroblast growth factor in cultured bovine aortic endothelial cells: Comparison with aminoguanidine 143–153

R. Reynoso, L.M. Salgado and V. Calderón: High levels of palmitic acid lead to insulin resistance due to changes in the level of phosphorylation of the insulin receptor and insulin receptor substrate-1 155–162

D.L. Santos, C.M. Palmeira, R. Seiça, J. Dias, J. Mesquita, A.J. Moreno and M.S. Santos: Diabetes and mitochondrial oxidative stress: A study using heart mitochondria from the diabetic Goto-Kakizaki rat 163–170

H. Rashid and S. Tayyab: Interaction of bilirubin with native and protein-depleted human erythrocyte membranes 171–177

Y. Gan, E. Taira, Y. Irie, T. Fujimoto and N. Miki: Arrest of cell cycle by Amida which is phosphorylated by Cdc2 kinase 179–185

M. Chmielewski, E. Sucajtys, J. Swierczynski, B. Rutkowski and W. Bogusławski: Arginine deprivation and tumour cell death: Arginase and its inhibition 187–191

G.A. Naderi, S. Asgary, N. Sarraf-Zadegan and H. Shirvany: Anti-oxidant effect of flavonoids on the susceptibility of LDL oxidation 193–196

Index to Volume 246 197–200

Molecular and Cellular Biochemistry **246:** 1, 2003.

Preface

Our vasculature is more than a simple conduit for carrying blood, it is a complex and dynamic organ system that affects every system in our bodies. The absolute requirement for a functioning circulatory system also means that its health impacts directly on our well being. It is for these reasons that there is so much interest directed at understanding how the vasculature functions in both healthy and disease states.

The articles in this volume examine all aspects of vascular biochemistry. Not only do they touch on the various tissue components present in the vascular wall, they also examine the hemodynamic and metabolic activities associated with its function. Why is this so important? It is well established that cardiovascular disease is the number one killer in the world. In the United States, 710,000 individuals died from heart disease in 2000, while across the world the death rate from heart disease is 17 million (1/3 of global deaths). Indeed, 12% of Americans have been diagnosed with heart disease, and this number increases to 35% for individuals over the age of 65. More significantly, coronary artery disease accounts for half of all cardiovascular conditions, and is the primary cause of heart attack and stroke. In addition, approximately 20% of individuals are hypertensive. These statistics clearly indicate the impact of vascular health on the general population. As well, there is a marked increase in the incidence of hypertension and coronary artery disease for diabetics. In fact, there is considerable support for the view that the cardiovascular consequences of diabetes occur as a result of vascular hyperreactivity. Since the incidence of diabetes is expected to increase from 4% to 5.4% of the total population between now and 2025, understanding the factors that influence vascular health will be necessary to develop the clinical tools needed to prevent a comparable increase in cardiovascular deaths.

The papers included in this volume represent research that is directed towards understanding vascular function. As well, many articles have examined the vasculature under conditions which mimic the various disease states described above. Atherosclerosis is considered in relation to lipid/cholesterol metabolism, infection, racial profiles and oxidation state. At the cellular level, the contribution of smooth muscle cell proliferation, gene expression and the activity of enzymes catalyzing cholesterol synthesis to atherosclerosis are considered. Similarly, hypertension is discussed in terms of vasoreactivity and endocrine responses. The significance of diabetes and autoimmune responses were also studied by contributors to this volume. As such, this volume presents a broad range of topics associated with vascular function.

The 27 manuscripts contained in this volume were contributed by scientists who had attended the XVII World Congress of the International Society for Heart Research held in Winnipeg, Canada in July, 2001. By participating in a Congress with almost 2000 attendees, the authors were able to provide new information for researchers that could have considerable impact on the future health of many individuals. The breadth of the work is also notable, since each of the pathological conditions associated with vascular disease typically has multiple causes. We therefore believe that the following articles will provide new insights into the mechanisms that control vascular function, as well as therapies designed to treat vascular disease.

Peter Zahradka, Jeffrey Wigle and Grant N. Pierce
St. Boniface General Hospital Research Centre
Winnipeg, Manitoba
Canada

Molecular and Cellular Biochemistry **246:** 3–11, 2003.

Osteoglycin expression and localization in rabbit tissues and atherosclerotic plaques

Borja Fernández,[1] Andreas Kampmann,[2] Frederic Pipp,[1] René Zimmermann[2] and Wolfgang Schaper[1]

[1]*Max-Planck-Institute, Department of Experimental Cardiology, Bad Nauheim;* [2]*Kerckhoff-Clinic, Vascular Genomics, Bad Nauheim, Germany*

Abstract

The localization of osteoglycin (OG), one of the corneal keratan sulfate proteoglycans, was studied in different normal rabbit tissues, as well as in atherosclerotic lesions, by means of *in situ* hybridization and immunohistochemistry. OG was associated with the vasculature of all the organs analyzed. Normal aortas showed abundance of the protein in the adventitia and focally in the media. Peripheral vessels showed OG localized only in the adventitia. OG mRNA was restricted to vascular smooth muscle cells, pericytes, and fibroblasts in aorta and skeletal muscle. In striated muscle, OG was abundant and distributed in foci around muscles and vessels, whereas in visceral muscle, the protein was homogeneously distributed throughout the extracellular matrix. In all the other organs studied, OG was only associated with the vasculature, with the exception of the lung and liver. In these two organs, the protein accumulated also around cartilage, alveoli, and hepatic duct. In atherosclerotic lesions, OG mRNA was down-regulated in the media and up-regulated in the activated endothelium and thick neo-intima, whereas the protein accumulated in the front edge of migrating smooth muscle cells. We conclude that OG is a basic component of the vascular extracellular matrix. OG also plays a role in atherosclerosis, and might be useful for therapeutic interventions. In addition, the possible involvement of OG in maintaining physical properties of tissues is discussed. (Mol Cell Biochem **246**: 3–11, 2003)

Key words: osteoglycin, keratan sulfate proteoglycans, mRNA and protein localization, rabbit tissues, vasculature

Introduction

Osteoglycin (OG), also called mimecan, is a keratan sulfate proteoglycan (KSPG) first isolated from bovine bone [1]. Later, it was found to be identical to an unidentified KSPG highly abundant in the cornea [2]. The OG core protein belongs to the small leucine-rich repeat protein (SLRP) family together with 20 other evolutionary conserved small interstitial proteoglycans [3]. SLRPs share three conserved domains [4]: (1) An amino-terminal domain containing negatively charged glycosaminoglycan chains, probably involved in binding to cell surface and extracellular matrix proteins. (2) A cysteine-free central domain with 8–10 tandem repeats of leucine-rich regions responsible for binding to type I collagen. (3) A carboxyl end domain that contains two cysteine residues with unknown function. The biological roles of SLRPs are most probably related to protein–protein interaction [4]. They are considered key regulators of collagen fibrillogenesis in skin and cornea [5]. In addition, members of the subfamily of SLRPs that includes OG have been shown to bind growth factors, especially members of the TGFβ superfamily, via the core protein [6].

KSPGs were initially characterized in three different tissues: cornea, cartilage and brain [7]. However, proteoglycans with similar antigenic and physical properties were also extracted from many different tissues, but with a limited distribution of keratan sulfate epitopes [8]. KSPGs are 10–20% as abundant in connective tissues as in the cornea [8], where they are responsible for corneal transparency by regulating collagen fibril structure [5, 9, 10]. Lumican, one of the cor-

Address for offprints: B. Fernández, Max-Planck-Institute, Department of Experimental Cardiology, Benekstrasse 2, D-61231 Bad Nauheim, Germany (E-mail: borjaf@kerckhoff.mpg.de)

neal KSPGs plays a similar regulatory role for fibrillogenesis in the skin [11]. No experimental evidence exists about the functions of KSPGs in tissues other than cornea and skin.

The distribution of OG, like other KSPGs, is widespread in many body tissues. It is highly abundant in cornea, sclera, and cultured kerationocytes, but it has also been detected at variable amounts in different organs [2, 12, 13]. However, the localization of OG in these tissues is mostly unknown. Only two studies have addressed OG protein or mRNA localization in tissues: OG protein has been detected in rat chondrocytes, osteocytes, and osteoblasts [14], whereas OG mRNA has been shown in normal and diseased arteries [15].

In the present study we have explored the localization of OG mRNA and protein in different organs, with special attention on vascular tissues. In addition, we have extended the previous observations of OG expression in rabbit atherosclerotic lesions. Our study is the first to describe the localization of OG in different organs, which may contribute to understanding the physiological functions of OG and KSPGs in health and disease.

Materials and methods

All animal studies were approved by the Bioethical Committee of the District of Darmstadt, Germany. Animals were handled in accordance with the American Physiological Society guidelines for animal welfare and the Guide for care and use of laboratory animals published by the US National Institutes of Health.

Normal tissues: aorta, skeletal muscle, heart, uterus, intestine, lung, liver, kidney, pancreas, spleen and brain were obtained from New Zealand White rabbits, and atherosclerotic lesions from Watanabe rabbits. All the animals were killed by an anesthetic overdose. For Northern and Western blot analyses, the tissues were rapidly collected, frozen in liquid Nitrogen, and stored at –80°C until use. For *in situ* hybridization, immunohistochemistry, and immunofluorescence the tissues were embedded in Tissue-teck mounting media (Sakura Finitek), and cryopreserved in liquid Nitrogen-cooled methyl butane (Merk).

Cloning of OG

OG was identified as clone AK47b2 in a Differential-Display-Reverse-Polymerase-Chain-Reaction (DDRT-PCR) screen for genes, which are differentially expressed during growth of arteries in rabbits (A. Kampmann *et al.*, paper in preparation). This clone showed homology to human OG (89%, Genbank Acc. No. NM014057). The full length cDNA (AK74b2 full length; submitted to Genbank) was amplified using the SMART 5′ RACE Kit (Clontech) and used as a probe for all further studies.

Northern blot

Total RNA was isolated from rabbit aorta and skeletal muscle according to the method of Chomczynski and Sacchi [16]. Northern blot hybridization was performed according to standard procedures [17] using the full length OG cDNA probe.

Western blot

Protein isolation and Western blot analysis were performed according to standard procedures [16]. In short, tissue was homogenized in extraction buffer (0.1 M Tris-HCl pH 8.0; 0.01 M EDTA; 0.04 M DTT; 10% (w/v) SDS) using an ultrasonic device (Sonoplus GM 70, Bandelin) and quantified using the Bio-rad assay. Equal amounts of proteins were then separated on precast 4–12% Tris-Gylcine gels (NOVEX). A polyclonal rat anti-OG antibody raised against a synthetic peptide from the N-terminus of the deduced rabbit OG amino acid sequence was used. Immunodetection was performed with an enzyme-linked chemiluminescence detection system (ECL-System; Amersham Pharmacia Biotech) and a peroxidase-conjucated goat anti-rat IgG secondary antibody (Santa Cruz).

In situ *hybridization*

Non-radioactive *in situ* hybridization was performed with digoxigenin-labeled mRNA probes, generated by the *in vitro* transcription method from the clone AK74b2 (full length). The RNA was labeled using the 'DIG RNA Labeling Mix' (Roche Diagnostic) as instructed by the supplier. The hybridization and detection protocols followed the 'Nonradioactive *in situ* hybridization application manual' (Roche Diagnostic). Briefly, cryosections were fixed in 4% paraformaldehyde, and washed first with phosphate buffer saline (PBS) and then with 2 × SSC (300 mM NaCl; 30 mM sodium citrate; pH 7.4). Prehybridization consisted of incubation with 4 × SSC + 50% formamide at 37°C for 20 min. Hybridization was performed overnight at 45°C with antisense or sense probes. After several 2× and 1 × SSC washing steps, sections were incubated with RNase A at 37°C for 30 min. Stringent washes consisted of: 2 × SSC + 50% formamide at 50°C; 1 × SSC at 37°C; 0.5 × SSC at room temperature, 10 min each. mRNA probes were detected with anti-digoxigenin antibodies conjugated with alkaline phosphatase as instructed.

Immunohistochemistry

Immunoperoxidase was performed in 5 or 10 μm cryosections. The sections were fixed with cooled acetone, air-dried and washed with PBS. After quenching the endogenous peroxidase activity with 3% hydrogen peroxide, the sections were washed in PBS, immersed in blocking solution (0.1% bovine serum albumin; 0.4% glycine in PBS) and incubated overnight with the rat polyclonal antibody against OG. After several PBS washing steps, the sections were incubated with a peroxidase-conjugated anti-rat IgG (Santa Cruz Biotechnology). Peroxidase was detected by incubation with 3,3′ diaminobenzidine (Sigma). The omission of the first antibody served as a negative control. In some sections, the nuclei were counterstained with hematoxilin. Photomicrographs were obtained with a Leica DMLD microscope.

In some cases, *in situ* hybridization with OG mRNA probes, or immunoperoxidase with OG antibodies were combined with immunofluorescence with vascular smooth muscle α-actin antibodies (FITC-conjugated anti-α-actin, *Sigma*) in consecutive cryosections. After the blocking step, the sections were incubated overnight with anti-α-actin antibodies and washed several times with PBS. Nuclei were counterstained with DAPI (Sigma).

Results

Northern blot analysis of tissue from rabbit aorta and skeletal muscle using clone AK74b2 (full length) revealed a single band of approximately 3.2 kb (Fig. 1A), corresponding well to the published mRNA size for rat OG [15]. Western blot results showed a major band at approximately 34 kDa in most organ tissues (Fig. 1B). This value corresponds to the predicted molecular weight of rat OG [15] and also to the predicted molecular weight of rabbit OG/AK74b2 (full length) (data not shown). Cardiac ventricles, uterus, and lung showed the strongest signals. Skeletal muscles, kidney, and brain also showed specific signals. In the liver and spleen, the signal was almost undetectable. The existence of multiple faint bands at higher molecular weight recognized by the antibody points to possible glycosylated forms of the protein.

In situ hybridization of normal rabbit aortas with antisense mRNA probes coding for OG revealed positive signals in the nuclei of smooth muscle cells of the arterial media and in adventitial fibroblasts (Figs 2A and 2B). The signal was homogeneously distributed in the media and was usually more abundant in the adventitia, whereas the endothelial cells were negative. Immunoperoxidase using anti-OG antibodies revealed focal deposits of the protein in the media and adventitia (Figs 2C and 2D). The localization of OG was extracellular, accumulating in the medial lamellae. The staining in adventitia was significantly more robust than in the media, showing a ring of immunoreactive material in the outer layer of the vessel. The endothelial layer and the subendothelial space were always devoid of protein.

In the quadriceps muscle, OG mRNA was located in the smooth muscle cells of the arteries, similar to the localization observed in the aorta (Fig. 3A). In addition, strong staining was found in tissue fibroblasts (Figs 3A and 3C), and in pericytes surrounding capillaries and small arterioles (Fig. 3B). Endothelial cells of capillaries, arteries and veins, as well as skeletal myocytes were negative. Immunoperoxidase staining of similar sections of the quadriceps muscle revealed a widespread distribution of OG protein in the extracellular matrix surrounding each muscle fiber (Fig. 4A). The signal decreased in intensity from the perimysium to the endomysium, with focal and patchy deposits of immunoreactive signal around individual myocytes (Fig. 4A). Strong OG staining was

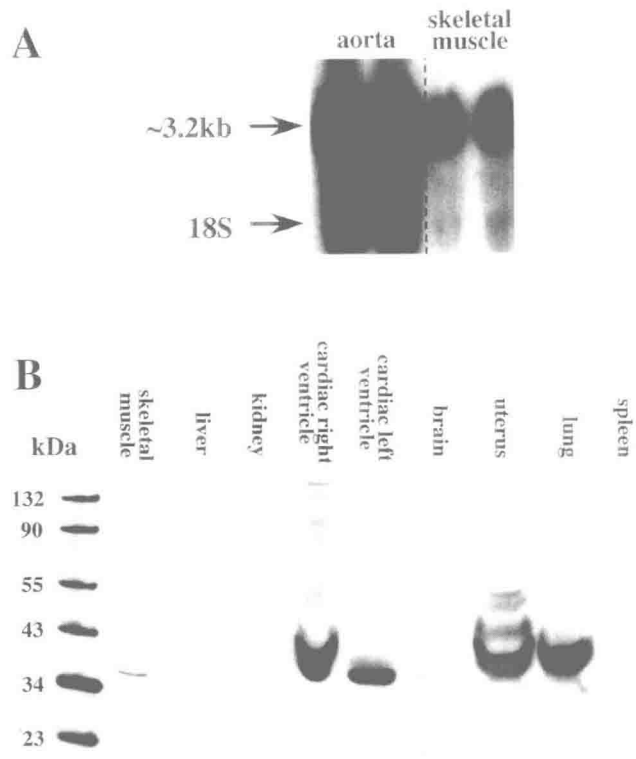

Fig. 1. (A) Northern blot analysis of OG in aorta and skeletal muscle. Hybridization to a single band of ≈ 3.2 kb is found. For reference, the size of the 18S rRNA is indicated. (B) Western blot showing the amount of OG protein in different rabbit organs. The polyclonal anti-OG antibodies recognized a major band of ≈ 34 kDa. The multiple faint bands recognized by the antibody point to possible glycosylated forms of the protein. Note that the secondary antibody used detects an epitope from the molecular weigh standard.

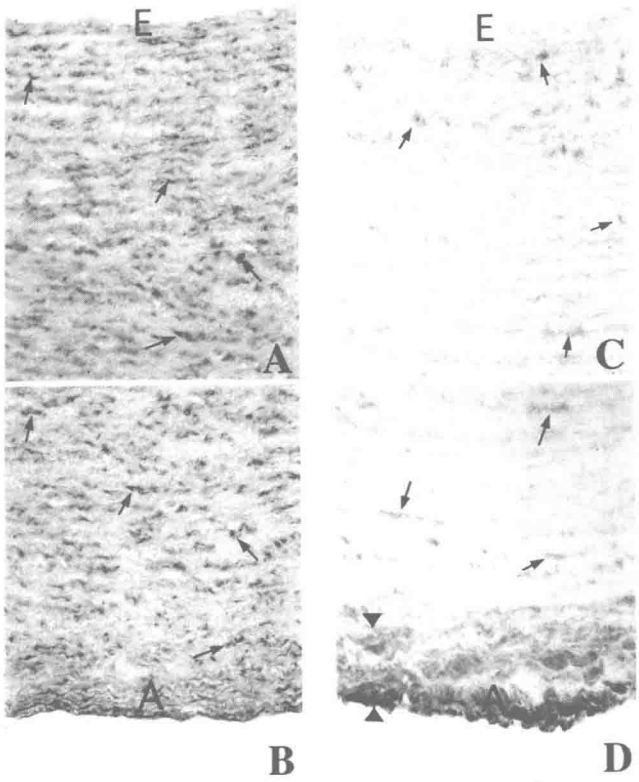

Fig. 2. In situ hybridization (A, B) and immunohistochemitry (C, D) of a normal rabbit aorta. A and C show the luminal part of the artery. B and D show the abluminal part. Arrows point to signals for OG mRNA (A, B), and OG protein (C, D) in the arterial media. The adventitia is indicated between arrowheads in D. A – adventitia; E – endothelium. (A–D: ×150).

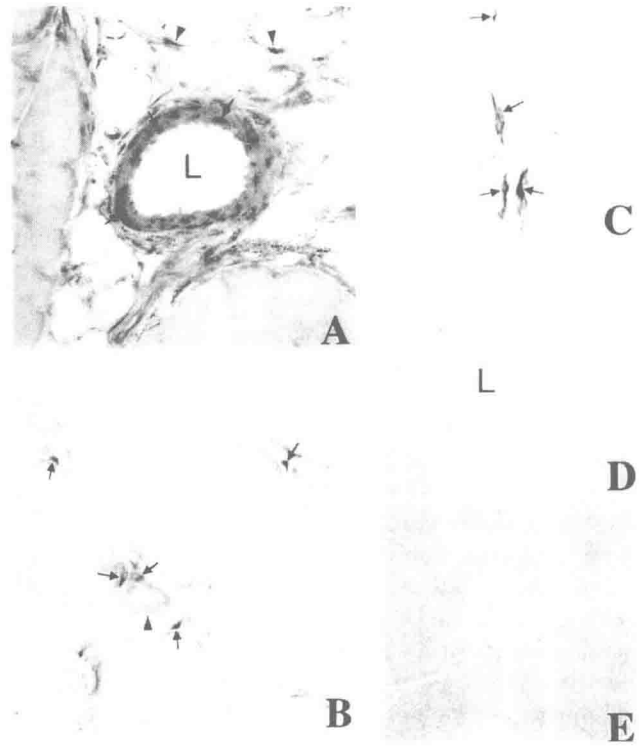

Fig. 3. In situ hybridization with OG mRNA antisense (A–C) and sense (D, E) probes of the quadriceps muscle. (A) Arrows indicate positive nuclei of arterial smooth muscle cells. Perivascular fibroblasts are also positive (arrowheads). (B) Positive pericytes (arrows) surround several capillaries and a small arteriole (arrowhead). Note that arteriolar endothelium, capillaries, and myocytes are negative. (C) Positive interstitial fibroblasts (arrows) are distributed among negative myocytes. (D, E) Incubation of the sections with a sense mRNA probe for OG resulted in no signal. L – lumen. (A: ×150; B: ×400; C: ×300; D: ×75; E: ×100).

observed around vessels. The protein accumulated in the adventitia of arteries and veins, but was always absent from the media and the endothelium (Fig. 4B).

In the heart, the pattern of OG immunostaining was found to be similar to that of skeletal muscles (Figs 4C and 4D). The protein was located in the extracellular matrix surrounding cardiomyocytes. The strongest staining was found in the subendocardium and subepicardium (Fig. 4C), as well as in the adventitia of the coronary vessels (Fig. 4D). The semilunar valves were also found to be immunoreactive (not shown).

In the uterus, the localization of OG was similar to that in the intestine (Fig. 5). However, it was found to be different compared to heart and skeletal muscles (compare Figs 4A and 4C with Figs 5A and 5C). Instead of patchy foci of immunoreactive material, a light brown staining was homogeneously distributed throughout the muscular, epithelial and vascular areas of both organs (Fig. 5). The protein intermingled with smooth muscle cell layers (Figs 5A–5C), and surrounded vessels of every size in the vascular areas (Figs 5B and 5D). OG also occupied the extracellular space around the intestinal and endometrial epithelia (Figs 5A–5C). In these two organs, no anatomical or histological structure was found to be more reactive than others to OG antibodies.

In the lung, the extracellular space beneath the bronchial epithelium was the richest in terms of OG immunoreactive content (Fig. 6A). The extracellular matrix surrounding the bronchial cartilage was also strongly immunoreactive. Dispersed foci of the protein were detected around the alveoli. The pulmonary vasculature showed a pattern of staining similar to that of the heart and skeletal muscle. However, the main pulmonary arteries and veins showed marked differences. In the pulmonary artery (Fig. 6B), OG concentrated in the adventitia, and was absent from the typically thick media of the vessel. In addition, a rim of the protein was found along the subendothelial surface. In the pulmonary vein, (Fig. 6C)

focal deposits of the protein were present in the medial lamellae, like in the aorta (Figs 2C and 2D) and vena cava (not shown). In the subendothelial space, OG formed a thick layer, not found in any other vessel studied.

In the liver, OG was associated with two histological structures: the hepatic duct, and the hepatic vasculature (Fig. 6D). In the hepatic duct, OG strongly concentrated around the epithelium. In the hepatic vasculature, the distribution of OG was similar to other organs. The portal vein, like other big veins showed focal depositions of OG not only in the adventitia, but in the media as well. (Fig. 6E).

In the kidney (Fig. 6F), brain, pancreas and spleen (not shown), the distribution of OG was exclusively restricted to the adventitia of the vessels. In these three organs, the parenchyma was completely devoid of any immunoreactive signal, and the distribution of OG around the vasculature was similar to that in other organs like the heart and skeletal muscle (Fig. 6F).

Given the prevalence of OG distribution in the vascular system, we studied OG mRNA and protein in the aortas of Watanabe rabbits with different degrees of atherosclerotic plaque development. Early stage is characterized by the formation of a thin neo-intima layer beneath the endothelium (Figs 7A and 7B). At this stage, the neo-intima consists of loosely arranged mesenchymal-like cells with no immunoreactivity to smooth muscle α-actin. While neo-intimal cells did not show any expression of OG mRNA, an ectopic expression was consistently detected in the endothelial cells covering the neo-intimal progression (Fig. 7A).

More advanced lesions showed a thick neo-intima layer composed of α-actin negative cells (Figs 7C–7E). OG mRNA expression disappeared from the endothelium, whereas the inner portion of the neo-intima (closer to the endothelium) acquired a strong staining (Fig. 7C). In addition, the inner part of the media that was composed of normally arranged α-actin positive smooth muscle cells without signs of elastica disruption (Fig. 7D), showed a consistent downregulation of OG mRNA (Fig. 7C). Immunohistochemical staining of OG in adjacent sections revealed accumulation of the protein in the intima layer, just beneath the location of OG expressing cells (Figs 7C and 7E).

End-stage lesions were characterized by the presence of a plaque composed of α-actin negative fibroblast-like cells (Figs 7F and 7G). The fibroblast-like cells were devoid of OG expression, whereas a thin rim of α-actin-negative cells surrounding the plaque showed clear positive signals (Fig. 7F).

Discussion

We used *in situ* hybridization and immunohistochemistry to examine for the first time the localization of OG mRNA and protein in rabbit organs. Our results confirm previous studies [2, 12, 13] demonstrating abundance of the protein in different tissues, and show a heterogeneous distribution of OG in different organs.

Despite differences in distribution among organs, the presence of OG in the vasculature is a constant histological feature in all the organs studied. *In situ* hybridization revealed that vascular smooth muscle cells, pericytes, and adventitial fibroblasts are the sources of OG in vessels, whereas endothelial cells do normally not express OG mRNA. Immunohistochemistry showed accumulation of the secreted protein in the adventitia of all arteries and veins. In peripheral vessels, OG is restricted to the adventitia, whereas in big arteries and veins, foci of OG were distributed also throughout the media. The endothelium and the subendothelial space are free of protein. Although the mRNA and protein localization of OG in the vasculature showed a consistent and constant pattern, the pulmonary vessels were found special in terms of its amount and distribution. The pulmonary arteries were the only normal big arteries with OG in the intima layer but not in the media, and the pulmonary veins also showed OG in the thick intima. Our immunohistochemical staining revealed accumulations of OG protein around big and medium size vessels. Yet, microvessels (arterioles, venules and capillaries) were usually not stained. This observation can be interpreted (1) as a restriction of the histological distribution of the protein or (2) as a limitation of the method due to low concentrations of the antigen. The later is more likely, because *in situ* hybridization revealed expression of OG mRNA by pericytes surrounding arterioles and capillaries. In any case, we can conclude that the proteoglycan OG is a basic component of the vascular extracellular matrix in all organs of the body.

There is only one study that showed OG mRNA expression by smooth muscle cells in the normal media of neonatal and adult aortas [15]. Other members of the LRSPs family have also been detected in vascular extracellular matrices: byglican is associated with intramural blood vessels of the uterus [4], and Decorin accumulates in the adventitia of mammary gland vessels [4]. In addition, Thieszen and Rosenquist [18] found that decorin interacts with collagen type III in the chick embryonic cardiac outflow tract. Our results, together with all these data strengthen the hypothesis that OG together with other SLRP family members are important in developing and maintaining the mature vascular extracellular matrix.

OG mRNA expression has been shown to be regulated in diseased arteries [15]. Therefore, we examined the localization of OG mRNA and protein in the aortas of Watanabe rabbits, a well-known model for atherosclerosis. In the early stages of intima formation, a consistent ectopic expression of OG was found in endothelial cells. During neo-intima progression, OG mRNA was up-regulated in the inner neo-intima and down-regulated in the inner media, whereas the

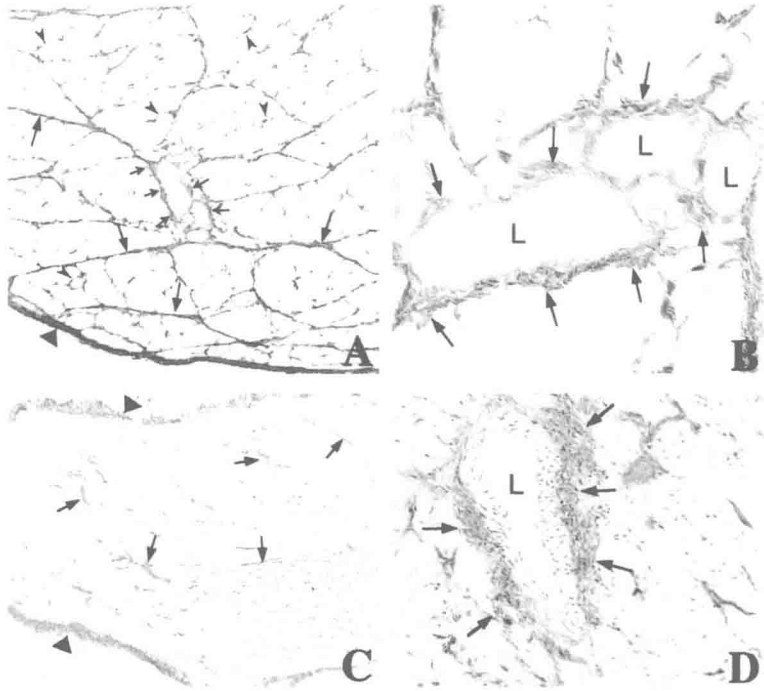

Fig. 4. OG immunohistochemical staining of rabbit quadriceps muscle (A, B) and heart (C, D). (A) A thick layer of immunoreactive OG surrounds the quadriceps muscle in the perimysium (big arrowhead). A smaller but continuous layer surrounds myofibers in the epimysium (big arrows). Focal deposits can be observed around individual myocytes in the endomysium (small arrowheads). Small arrows point to the adventitia of arteries. (B) Higher magnification of the arteries shown in A. OG accumulates in the adventitia (arrows). (C) In a papillary muscle of the heart, a thick layer of OG accumulates in the epicardium (arrowheads). Thick and focal deposits of OG are visible in the myocardial interstitium (arrows). (D) A coronary artery is surrounded by abundant immunodetectable OG. L – lumen. (A: ×90; B: ×300; C: ×50; D: ×200)

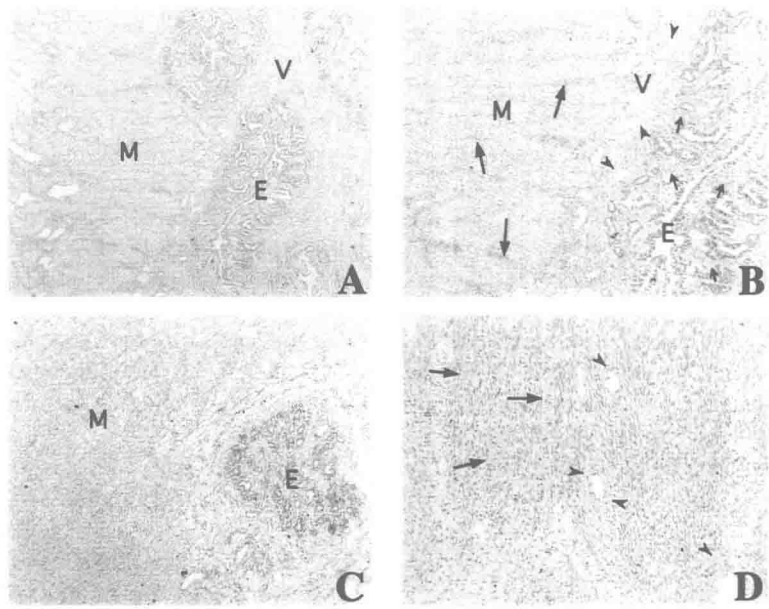

Fig. 5. OG immunohistochemical staining of rabbit intestine (A, B) and uterus (C, D). A light and homogeneous staining can be observed in the muscular (M), epithelial (E), and vascular (V) areas of both, intestine and uterus. Big arrows point to OG around smooth muscle cells, small arrows around epithelial cells, and arrowheads around vessels. (A, C: ×50; B, D: ×100).

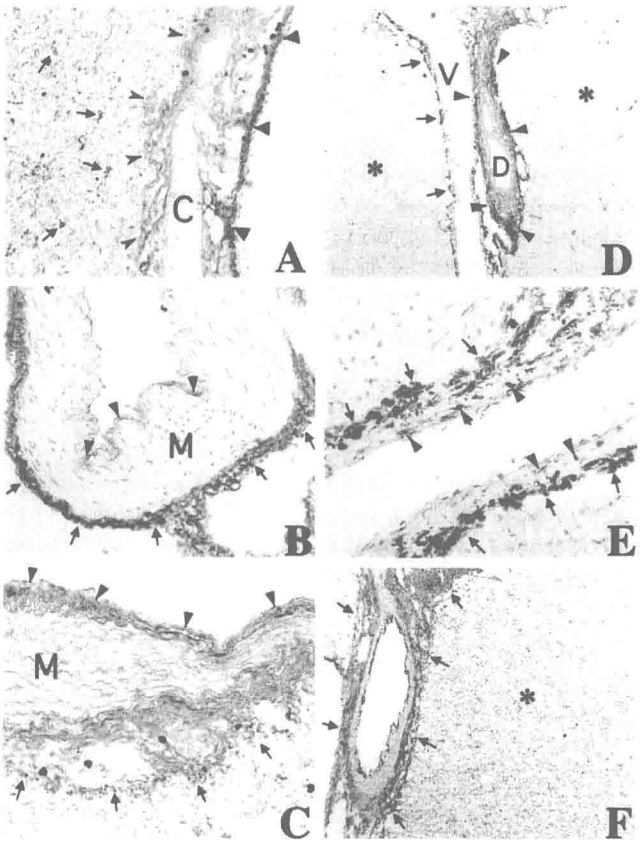

Fig. 6. OG immunohistochemical staining of rabbit lung (A–C), liver (D, E), and kidney (F). (A) OG forms a thick layer beneath the bronchial epithelium (big arrowheads). Small arrowheads point to OG surrounding cartilaginous tissue. Focal deposits of the protein associate with the lung alveoli (arrows). (B) A pulmonary artery shows strong OG immunorreactivity in the adventitia (arrows). OG forms a thin but detectable rim beneath the arterial endothelium (arrowheads). (C) In a pulmonary vein, OG accumulates in the adventitia (arrows), media (M), and intima (arrowheads). (D) The liver parenchyma is devoid of OG staining (asterisks). Arrowheads and arrows point to OG deposits around the hepatic duct and portal vein respectively. (E) In the portal vein, OG is present in the adventitia (arrows) and media (arrowheads). F: the parenchyma of the kidney is free of OG (asterisk), whereas the adventitia of an artery shows a strong staining (arrows). C – cartilage; D – hepatic duct; M – media; V – portal vein. (A, D, F: ×50; B, C, E:

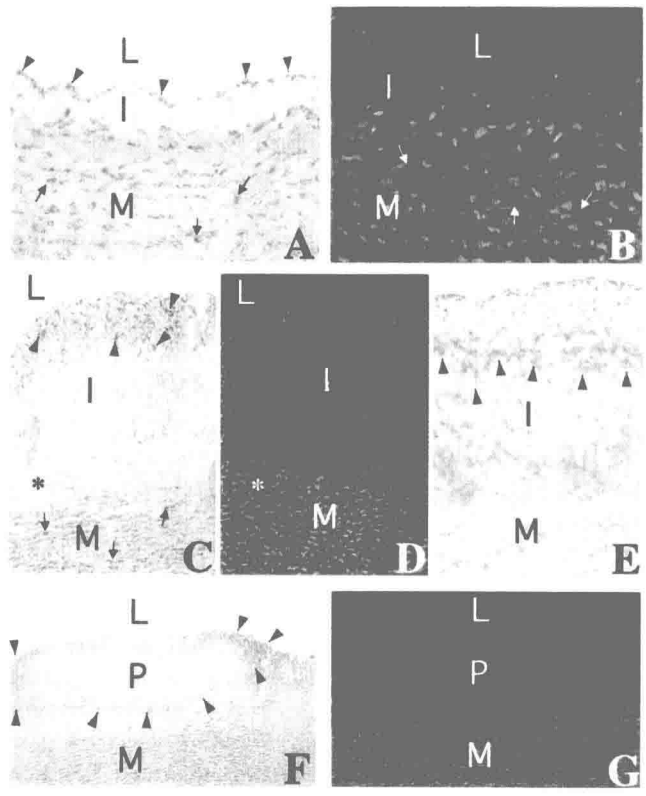

Fig. 7. In situ hybridization for OG (A, C, F), immunohistochemistry for OG (E), and immunofluorescence for vascular smooth muscle a-actin (B, D, G) of Watanabe atherosclerotic lesions. (A, B) Consecutive sections of an early lesion. Alpha-actin-positive smooth muscle cells of the media (arrows in B) show a normal OG mRNA expression pattern (arrows in A; compare with Fig. 1A). OG mRNA is also clearly detectable in the endothelium (arrowheads), but not in the neo-intima (I). (C–E): Consecutive sections of an advanced lesion. A thick neo-intima with α-actin-negative cells (I in D) shows OG mRNA expression only in the cells close to the lumen (arrowheads in C). The α-actin-positive smooth muscle cells at the inner part of the media (asterisk in D) show no OG mRNA signal (asterisk in C). OG protein accumulates in the neo-intima, just beneath the OG expressing cells (arrowheads in E). (F, G) Consecutive sections of an end stage lesion. The cells of the fibrous plaque are devoid of α-actin protein and OG mRNA (P in G and F respectively). The cells surrounding the plaque show some OG expression (arrowheads in F). I – neo-intima; L – lumen; M – media; P – plaque. (A, B: ×150; C–E: ×75; F, G: ×50).

protein accumulated in the intima. End stage atherosclerotic lesions showed no OG expression in the fibrous plaque, but an up-regulation in the cells surrounding the plaque was observed. Our results mainly support those from Shanahan and collaborators [15] obtained in injured carotid and atherosclerotic coronary arteries. The localization of OG mRNA in the neo-intima of advanced lesions is of special interest. Both, the study of Shanahan and ours revealed expression of OG in neo-intimal cells close to the lumen, whereas medial smooth muscle cells close to the neo-intima showed a clear down-regulation. In addition, our immunohistochemical study indicates that the secreted protein accumulates beneath the OG expressing cells, forming a lamina of immunoreactive material (Fig. 7E). These results suggest that the protein forms a border for the smooth muscle cells (not expressing OG) migrating from the media (Figs 7C–7E). Whether OG is implicated in the migration of medial smooth muscle cells during the progression of vascular disease remains to be confirmed. Another relevant finding of our study is the consistent expression of OG mRNA by activated endothelial cells

as an early event during atherosclerotic progression. This expression pattern is ectopic because endothelium was never found positive in any normal tissue. Although the biological significance of this finding is unknown, the early expression in a relatively accessible cell type makes OG an attractive candidate for possible preventive therapeutic interventions.

The organs analyzed in the present study can be divided into three groups, based on the amount and distribution of OG in their extracellular matrices. (1) Striated muscles (heart and skeletal muscle): abundant foci of OG in the extracellular space, not exclusively associated with the vasculature but with myocytes as well. (2) Visceral smooth muscle tissues (uterus and intestine): abundance of OG distributed not in foci, but homogeneously around all the extracellular spaces. (3) Non-muscular tissues (kidney, brain, and pancreas): OG located exclusively around the vasculature, associated with the adventitia of vessels. One exception is the lung. This is the only non-muscular organ studied where OG is abundant and associated with different histological structures including the epithelium, the cartilage, and the alveoli. The accumulation of OG in the portal duct is another remarkable feature. Our study confirms previous data showing a widespread distribution of SLRPs in many organs. However, the histological localization of only three members of the protein family is currently known in a limited number of organs. Biglycan protein is abundant in the epidermis and follicular epithelium of the mammary glands [4]. In the uterus, biglycan surrounds the glandular epithelium and intramural blood vessels, similar to the distribution of OG showed in the present study. Decorin is also abundant in the skin [4], and its localization in skeletal muscles and vasculature coincides with that of OG presented here. Moreover, decorin localization in chick aortic arch vessels shows high homology to OG localization in rabbit aortas [18]. OG antibodies have been found to react with chondrocytes, osteocytes, and osteoblasts in rat forelimbs [14], but no other histological structure was examined in that study. The study of Shanahan [15] however, showed a localization of OG mRNA in arteries similar to that presented here. Taken together, all these results show a coincident localization of structurally related SLRPs in tissues. We can hypothesize then that structurally related SLRPs have similar physiological roles in those tissues. The functions of these SLRPs are most probably related to protein–protein interactions, more precisely to collagen fibrillogenesis. This assumption arrives from several biochemical, *in vitro*, and *in vivo* studies [4, 5, 9–11, 19–21]. These studies suggest that the function of SLRPs such as decorin, lumican, proteoglycan-Lb, and OG is to keep the spatial order of collagen fibers. This molecular function of SLRPs may determine physical properties of tissues such as elasticity and tensile strength. Indeed, a deficit in the lumican gene causes skin laxity and fragility in mutant mice [11]. In addition decorin, a dermatan sulfate proteoglycan with a high sequence homology to OG, has been demonstrated to interact with collagen type III in order to stabilize the large helical configuration of the aortic arch arteries [18]. In our study, abundance of OG was restricted to anatomical structures where tension and elastic forces play a crucial role, like uterus, intestine, muscles, lung, ducts, and vessels. In this regard, the unique distribution of OG in the pulmonary vasculature, which must adapt to significant physiological changes in flood blow, has special relevance. Therefore, it is tempting to speculate that OG is implicated in the regulation of elastic properties of organs.

Acknowledgements

We thank Professor Dr. Jutta Schaper and Dr. Sawa Kostin for their invaluable advice and suggestions in the morphological evaluations. We thank also Kerstin Wiczorek, and Claudia Ullmann for technical assistance, and Geard Staemmler for his help in editing pictures and text.

References

1. Bentz H, Nathan RM, Rosen DM, Armstrong RM, Thompson AY, Segarini PR, Mathews MC, Dasch JR, Piez KA, Seyedin SM: Purification and characterization of a unique osteoinductive factor from bovine bone. J Biol Chem 264: 20805–20810, 1989
2. Funderburgh JL, Corpuz LM, Roth MR, Funderburgh ML, Tasheva ES, Conrad GW: Mimecan, the 25-kDa corneal keratan sulfate proteoglycan, is a product of the gene producing osteoglycin. J Biol Chem 272: 28089–28095, 1997
3. Blochberger TC, Vergnes J-P, Hempel J, Hassells JR: cDNA to chick Lumican (corneal keratan sulfate proteoglycan) reveals homology to the small interstitial proteoglycan gene family and expression in muscle and intestine. J Biol Chem 267: 347–352, 1992
4. Danielson KG, Baribault H, Holmes DF, Graham H, Kadler KE, Iozzo RV: Targeted disruption of decorin leads to abnormal collagen fibril morphology and skin fragility. J Cell Biol 136: 729–743, 1997
5. Rada JA, Cornuet PK, Hassell JR: Regulation of corneal collagen fibrillogenesis *in vitro* by corneal proteoglycan (lumican and decorin) core proteins. Exp Eye Res 56: 635–648, 1993
6. Yamaguchi Y, Mann DM, Ruoslahti E: Negative regulation of transforming growth factor-β by the proteoglycan decorin. Nature 346: 281–284, 1990
7. Krusius T, Finne J, Margolis RK, Margolis RU: Identification of an O-glycosidic mannose-linked sialylated tetrasaccharide and keratan sulfate oligosaccharides in the chondroitin sulfate proteoglycan of brain. J Biol Chem 261: 8237–8242, 1986
8. Funderburgh JL, Caterson B, Conrad GW: Distribution of proteoglycans antigenically related to corneal keratan sulfate proteoglycan. J Biol Chem 262: 11634–11640, 1987
9. Scott JE: Proteoglycan-fibrillar collagen interactions. Biochem J 252: 313–323, 1988
10. Vogel KG, Paulsson M, Heinegard D: Specific inhibition of type I and type II collagen fibrillogenesis by the small proteoglycans of tendon. Biochem J 223: 587–597, 1984

11. Chakravarti S, Magnuson T, Lass JH, Jepsen KJ, LaMantia C, Carroll H: Lumican regulates collagen fibril assembly: Skin fragility and corneal opacity in the absence of lumican. J Cell Biol 14: 1277–1286, 1998
12. Corpuz LM, Funderburgh JL, Funderburgh ML, Bottomley GS, Prakash S, Conrad GW: Molecular cloning and tissue distribution of keratocan. J Biol Chem 271: 9759–9763, 1996
13. Tasheva ES, Corpuz LM, Funderburgh JL, Conrad GW: Differential splicing and alternative polyadenylation generate multiple mimecan mRNA transcripts J Biol Chem 272: 32551–32556, 1997
14. Dash JR, Pace DR, Avis PD, Bentz H, Chu S: Characterization of monoclonal antibodies recognizing bovine bone osteoglycin. Conn Tissue Res 30: 11–21, 1993
15. Shanahan CM, Cary NRB, Osbourn JK, Weissberg PL: Identification of osteoglycin as a component of the vascular matrix. Differential expression by vascular smooth muscle cells during neointima formation and in atherosclerotic plaques. Arterioscl Thromb Vascular Biol 17: 2437–2447, 1997
16. Chomczynski P, Sacchi N: Single-step method of RNA isolation by acid guanidinium thiocyanate-phenol-chloroform extraction. Anal Biochem 162: 156–159, 1987
17. Sambrook J, Fritsch EF, Maniatis T: Molecular Cloning: A Laboratory Manual. Cold Spring Harbor Laboratory Press, New York, 1989
18. Thieszen SL, Rosenquist TH: Expression of collagens and decorin during aortic arch artery development: Implications for matrix pattern formation. Matrix Biol 14: 573–582, 1994
19. Scott JE, Orford CR: Dermatan sulphate-rich proteoglycan associates with rat tail-tendon collagen at the d band in the gap region. Biochem J 197: 213–216, 1981
20. Hedbom E, Heinegard D: Binding of fibromodulin and decorin to separate sites on fibrillar collagens. J Biol Chem 268: 27307–27312, 1993.
21. Schonherr E, Hausser H, Beavan L, Kresse H: Decorin-type I collagen interaction. J Biol Chem 270: 8877–8883, 1995